



Fluorometric determination of nitrite through its catalytic effect on the oxidation of iodide and subsequent etching of gold nanoclusters by free iodine

Zhu Su¹ · Xinyi Wang¹ · Minchuan Luo¹ · Liang Li² · Yifeng Tu¹ · Jilin Yan¹

Received: 25 March 2019 / Accepted: 1 August 2019 / Published online: 13 August 2019
© Springer-Verlag GmbH Austria, part of Springer Nature 2019

Abstract

A method for sensitive detection of nitrite is presented. It is found that the red fluorescence of gold nanoclusters (with excitation/emission maxima at 365/635 nm) is quenched by traces of iodine via etching. Free iodide is formed by oxidation of iodide by bromate anion under the catalytic effect of nitrite. This catalytic process provides a sensitive means for nitrite detection. Under the optimal conditions, fluorescence linearly drops in the 10 nM to 0.8 μM nitrite concentration range. The limit of detection is 1.1 nM. This is a few orders of magnitude lower than the maximum concentration allowed by authorities.

Keywords Nitrite · Gold nanocluster · Fluorescence quenching · Iodine · Water samples · Kinetic fluorescence

Introduction

In biology, nitrite plays an important role in the generation of nitric oxide (NO) and other bioactive nitrogen oxides that are crucial for blood flow regulation, cell signaling and responses to hypoxia [1]. In food industry, nitrite is capable of inhibiting the growth of some bacteria, as well as giving meat an attractive color [2, 3]. However, blood red cells are combined with nitrite, which results in a decreased ability of carrying oxygen. Intake of unusually high amount of nitrite will lead to methemoglobinemia, with related symptoms like blood pressure decrease, heart rate increase, and even death in some cases [4]. Recent studies also show that under acidic conditions (e.g. as in gastric juice), this species can be converted into N-nitroso

compounds related to cancer, and thus is listed as “probably carcinogenic to human” by the World Health Organization (WHO) [5, 6]. Strict regulations should be observed in the applications of this species in food industry and other fields. Monitoring of nitrite is usually performed with ion chromatography [7], photometry [8], fluorescence [9], electrochemistry [10], etc. In these detection schemes, sensitivity or selectivity is sometimes a problem, and usually complicated processes or instrumentations are required. Therefore, further development of detections with higher performances would be great interest in the field of analysis.

Fluorescent measurements are now among the schemes providing the highest sensitivity. For their advantageous characteristics such as high luminescence, good stability and compatibility, nano-sized materials are frequently adopted in the fluorescent analyses [11]. Gold nanoclusters (AuNCs) are a type of ultra-small entities, and metallic cores comprise limited number (a few to tens) of gold atoms. Some of these AuNCs are highly luminescent under suitable radiations, and thus are applied in the construction of various fluorescence probes. Most of these detection methods are based on direct interaction of the targets with the AuNCs, such as those from copper ion, hydrogen peroxide, mercury, etc. [12, 13]. These interactions provide one-to-one signal from the processes, and usually limited sensitivities are rendered [14].

Instead of one-to-one scheme, a popular strategy in analysis is based on catalysis. The introduction of a catalyst brings

Electronic supplementary material The online version of this article (<https://doi.org/10.1007/s00604-019-3729-6>) contains supplementary material, which is available to authorized users.

✉ Jilin Yan
yanjl@suda.edu.cn

¹ The Key Lab of Health Chemistry and Molecular Diagnosis of Suzhou, College of Chemistry, Chemical Engineering and Materials Science, Soochow University, 199 Ren'ai Road, Industrial Park, Suzhou 215123, China

² School of Materials Science and Engineering, Wuhan Institute of Technology, Wuhan 430205, China

in multiple responses and usually much improved sensitivity can be obtained [15]. In this work, nitrite ion itself was found capable of catalyzing an oxidation reaction, and this property was coupled to the characteristic of the gold nanoclusters. Due to the cycling of nitrite in the catalytic process, a fluorescent kinetic assay was developed for nitrite measurement. This scheme rendered a limit of detection down to the nanomolar level.

Materials and methods

Chemicals and materials

Chloroauric acid tetrahydrate ($\text{HAuCl}_4 \cdot 4\text{H}_2\text{O}$), potassium bromate (KBrO_3), sodium nitrite (NaNO_2) and potassium iodide (KI) were purchased from Sinopharm Chemical Reagent Co., (Shanghai, China <http://www.shreagent.com/>). Bovine serum albumin (BSA) was from Suzhou Yacoo Chemical Co., (Suzhou, China <http://www.yacoo.com.cn/>). All other chemicals were of analytical grade and used as received. Double-distilled water was used throughout the procedure.

Instruments and apparatuses

Fluorescence signals were obtained on an F-2500 fluorospectrophotometer (Hitachi, Japan <http://www.hitachi.com/>) with a xenon lamp excitation. The slit widths of both excitation and emission were kept at 10 nm and 20 nm respectively, and a bias voltage of 700 V was applied onto the photomultiplier tube (PMT). Ultraviolet-visible absorption spectra were measured with a TU-1900 UV-vis spectrophotometer (PGeneral Instruments, China, <http://www.pgeneral.com/>). Microscopic images of the nanoclusters were taken under a Tecnai G220 transmission electron microscope (TEM, 200 kV) (FEI, Unites States, <http://www.fei.com/>). Dynamic Light Scattering spectrum was measured with a BI-200SM laser light scattering spectrometer (DLS, 22 mW) (Brookhaven, Unites States, <https://www.brookhaveninstruments.com/>).

Synthesis of the nanoclusters

Gold nanoclusters were synthesized with a one-pot reduction [16]. In this process, the protein BSA functioned as both the reducing agent and the stabilizer (the detailed description of the synthesis was provided in the Electronic Supporting Material (ESM)).

Fluorescence detections

All detections were performed under room temperature. The gold nanoclusters synthesized above were first diluted 30-fold

with double-distilled water. In 1.5 mL centrifuge tubes, 100 μL nitrite samples at various concentrations were respectively mixed with both 120 μL sulfuric acid ($0.01 \text{ mol}\cdot\text{L}^{-1}$) and 50 μL potassium bromate ($0.01 \text{ mol}\cdot\text{L}^{-1}$). Then 150 μL iodide ($0.01 \text{ mol}\cdot\text{L}^{-1}$) was added into the tubes, and the mixtures were diluted to 1 mL with double-distilled water. After 60 min incubation, an aliquot of 100 μL of the diluted AuNCs was then added to the mixtures. After another 15 min incubation, the mixtures were taken for related fluorescence measurements, and fluorescent intensities at 635 nm were collected under the 365 nm excitation.

Results and discussions

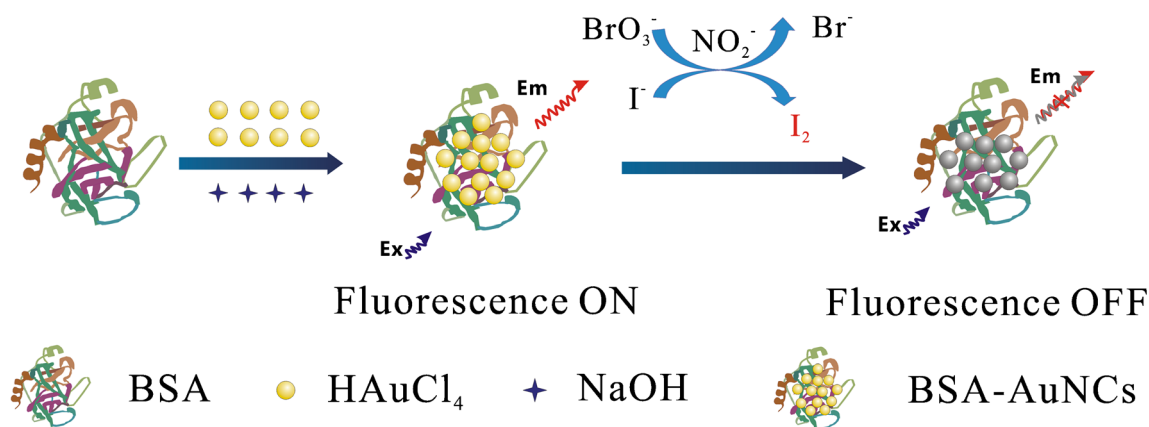
Gold nanoclusters and its direct responses toward nitrite

Among the nano-sized fluorescence probes, gold nanoclusters can be conveniently synthesized through a one-pot process [16]. Under an alkaline condition, BSA reduced trivalent gold into atoms, while at the same time this protein stabilized the so-formed metallic core. From the transmission electron microscope image (Fig. S1) and the dynamic light scattering spectrum (Fig. S2), these nanoclusters were found with diameter around 2.5 nm. In the UV-vis spectra as compared with bare BSA, a new absorption peak showed up around 365 nm (Fig. S3). Once excited, emissions were found with maxima at 440 and 635 nm respectively.

This kind of nanocluster has been intensively reported for sensing various targets, from small ions to large biomolecules as proteins and DNAs [17, 18]. The most popular route for these detection methods are based on the interaction between the targets and the nanoclusters. Reactions with either the metallic cores or the stabilizers often lead to fluorescence spectrum change (increase, decrease in the intensities or the peak shift), and the changes are applied in the subsequent quantification of the analyte. Some reported showed that nitrite ion directly quenched the AuNC fluorescence [19], however, for the AuNCs here, such kind of response was not observed: upon applying a nitrite sample with relatively high concentration onto our nanoclusters, no obvious fluorescence change was found (Fig. S4).

Detection of nitrite through catalysis

Instead of direct interaction, catalytic reactions are promising by virtue of bringing in multiple responses and amplified signals. One example is ELISA (enzyme linked immunosorbent assay) for immunoassays: the incorporation of an enzyme through the antibody-antigen reaction allows for further catalysis of the substrate and generation of amplified signals. In order to construct a similar design, it was better to make nitrite

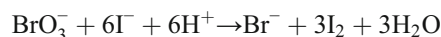


Scheme 1 Illustration of the nitrite detection.

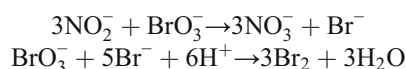
function as the catalyst for some specific reactions. For the target reaction to be catalyzed, the iodide-to-iodine conversion ($\text{I}^- \rightarrow \text{I}_2$) was a good candidate. This redox couple ($\text{I}_2 + 2\text{e}^- \leftrightarrow 2\text{I}^-$ $E^\circ = 0.54$ V) comes with a good reversibility and has been widely applied in analytical chemistry (iodimetry and iodometry). Our previous results showed that the BSA-AuNC fluorescence is not affected by iodide, but iodine combines with iodide and formed a powerful etchant (I_3^-/I^-) toward gold atoms (inside the metallic core of the AuNCs). This etching comes from the oxidative property of iodine together with the strong binding from iodide as a ligand [15]. Because of the high dependency of the nanoclusters' fluorescence on their metallic cores, this etching brings about a significant fluorescence quenching [16]. This kind of response provides a sensitive means for iodine detection, and has been applied in related substance measurement. If nitrite catalyzes this kind of reaction, an amplified response might be achieved with an

improved sensitivity. From some other reports, similar catalysis did happen with nitrite [20]. For the desired iodide-to-iodine conversion, an oxidant was required. Different candidates were tested, and bromate (BrO_3^-) was found suitable [21, 22]. Neither bromate or iodide were found with significant influence on the AuNC fluorescence (Fig. S5). Before applying onto gold nanoclusters, iodide-bromate solutions with and without nitrite were compared. After 60 min incubation, the one with nitrite gave a pale brown color (from the elemental iodine generated), while the one without nitrite did not (figure not shown). The production of iodine was also visualized with the subsequent dark-blue color through an introduction of starch (Fig. S6). This large difference came from the rather limited reaction rate between bromate and iodide under the experimental condition, as well as the catalysis from nitrite. Because of the small amount of nitrite added (10 μM , while both iodide and bromate were at mM level), it indicated that a sensitive detection was possible through this strategy.

In this reaction, bromate functioned as the oxidizing agent toward iodide, ($\text{Br}_2 + 2\text{e}^- \rightarrow 2\text{Br}^-$ $E^\circ = 1.08$ V), and iodine (I_2) was generated with a total reaction as:



Under the strong oxidant bromate, nitrite ion was first oxidized into nitrate [23]:



The subsequent oxidation of iodide generated the iodine required for the nanocluster etching, while nitrate was reverted into nitrite through the reduction from iodide:

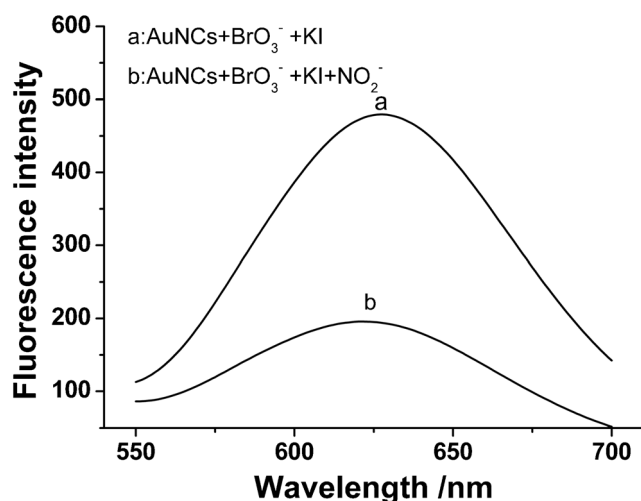
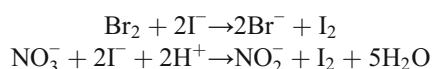
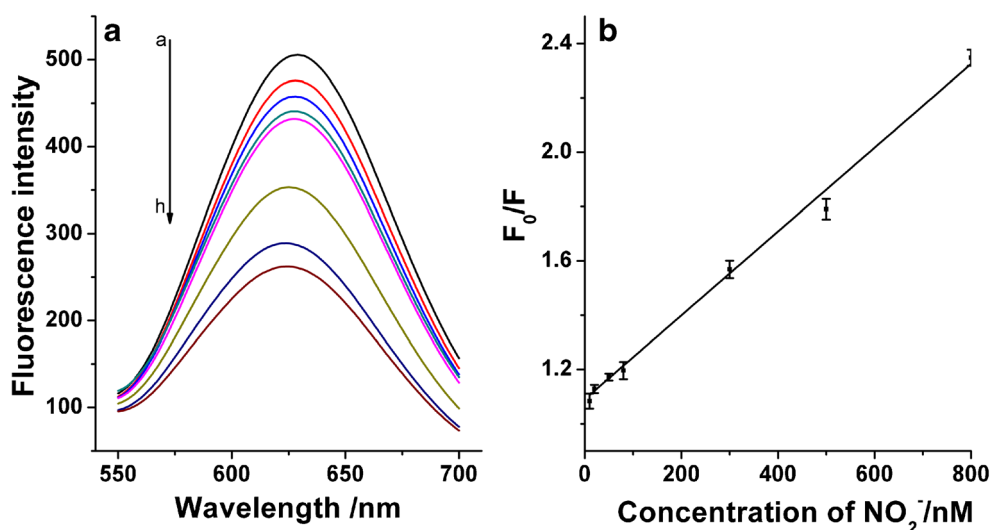


Fig. 1 Fluorescence spectra of the gold nanoclusters without (a) and with 1 μM NO_2^- (b). 0.5 mM KBrO_3 and 1.0 mM KI in 1.2 mM H_2SO_4 were first incubated with/without nitrite for 60 min. The mixtures were then applied onto AuNCs for 30 min incubation. The fluorescence responses were obtained with 365 nm excitation

Fig. 2 **a** Fluorescence responses to NO_2^- samples at different concentrations (from a to h: 0, 10, 20, 50, 80, 300, 500, 800 nM NO_2^-). **b** The Stern-Volmer plot of the fluorescence quenching. Nitrite samples were first incubated with 0.5 mM KBrO_3 and 1.5 mM KI under 1.2 mM H_2SO_4 for 60 min, and then the produced mixtures were applied onto AuNCs for 15 min incubation. The fluorescence responses were obtained with 365 nm excitation



During such a kind of process, nitrite ions accelerated the oxidation of iodide into iodine.

For the catalytic property of nitrite in the above iodine generation process, it was possible to construct a method for nitrite detection (Scheme 1). In this design, with excessive reactants (bromate and iodide), nitrite recycled for a continuous production of iodine, and the further interaction with AuNCs would bring in quenching as the fluorescence signal.

Upon applying bromate-iodide samples with and without nitrite onto gold nanoclusters respectively, an obvious difference occurred between the fluorescence spectra of related nanoclusters. As compared the one where nitrite was absent, the one with nitrite rendered a much enhanced fluorescence

quenching (Fig. 1). This large difference was further taken for nitrite analysis.

Optimization of the experimental conditions

The following parameters were optimized: (a) Kind of acid; (b) concentration of sulfuric acid; (c) concentration of iodide; (d) concentration of potassium bromate; (e) catalytic time and incubation time. Respective text and Figures on optimizations are given in the Electronic Supporting Material (FigS7-S11). In short, the following experimental conditions were found to give best results: (a) Best acid: sulfuric acid; (b) Best sulfuric acid concentration: 1.2 mM; (c) Best iodide concentration:

Table 1 Analytical performances of different detection schemes

Detection material	Linear range	Limit of detection	Reference
Electrochemistry			
$\text{CaFe}_2\text{O}_4(\text{CFO})$ clusters	0.016–1921 mM	6.6 nM	[24]
NiHCF/PDAP	0.1–130 μM	0.0151 μM	[25]
AuCuNCNs	0.01–4.0 mM	0.2 μM	[26]
Spectrophotometry			
$\text{Ru}(\text{npy})([\text{9}] \text{janeS3})(\text{CO})(\text{ClO}_4)$	1–840 μM	0.39 μM	[27]
Fluorimetry			
N-CQDs	0.2–20 μM	40 nM	[28]
N-CNDs	0–1.0 mM	1.0 μM .	[29]
PEI-CdS QDs	0.1–100 μM	65 μM	[30]
PA	0.1–10 μM	43 nM	[31]
CQDs	10–400 μM	0.48 μM	[32]
DAFFM DA	0.5–1.5 μM	33 nM	[33]
BSA-AuNCs	10–800 nM	1.1 nM	This work

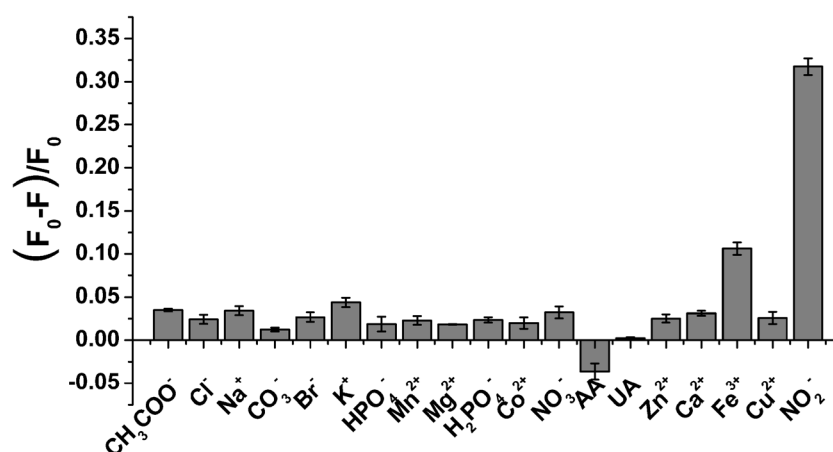


Fig. 3 Fluorescence quenching from different species. The concentration of NO_2^- was 100 nM, while that of Cl^- , Na^+ , CO_3^{2-} , Br^- , CH_3COO^- , HPO_4^{2-} , H_2PO_4^- , NO_3^- , K^+ , Mn^{2+} , Mg^{2+} , Co^{2+} , ascorbic acid (AA) and uric acids (UA) were 10 μM , Zn^{2+} and Ca^{2+} were 2 μM , Fe^{3+} and Cu^{2+} were 1 μM . Samples were first incubated with 0.5 mM KBrO_3 and

1.5 mM KI under 1.2 mM H_2SO_4 for 60 min, and then the produced mixtures were applied onto AuNCs for 15 min incubation. All fluorescence responses were obtained with 365 nm excitation and collected at 635 nm

1.5 mM; (d) Best potassium bromate concentration: 0.5 mM; (e) Best catalytic time and incubation time: 60 min, 15 min.

Analytical performances

Nitrite samples at different concentrations were measured with the developed method (Fig. 2a). Through related Stern-Volmer plot, the quenching efficiency is found linear to the NO_2^- concentration from 10 nM to 0.8 μM , the linear regression formula is $F_0/F = 1.09085 + 0.00154 [\text{NO}_2^-]$ (where F and F_0 were the fluorescence intensities in the absence and presence of nitrite respectively) with a correlation coefficient $R^2 = 0.9961$ (Fig. 2b). The limit of detection (LOD) of the method is estimated to be 1.1 $\text{nmol}\cdot\text{L}^{-1}$ ($\text{LOD} = 3\sigma_b/b$, where σ_b is the standard deviation of the blank samples and b is the slope of the Stern-Volmer plot). This value is a few orders of magnitude lower than the maximum contaminant levels in drinking water regulated by U.S. Environmental Protection Agency (EPA) (1 $\text{mg}\cdot\text{L}^{-1}$ as N, approximately 70 μM of nitrite). Also, this performance is among the best from previous reports (Table 1) [24–33]. To test the reproducibility of the detection, seven replicate measurements of a NO_2^- sample at 10 nM were performed. The relative standard deviation (RSD)

from the result (1.49%) indicates an excellent repeatability of the detection scheme.

To verify the specificity, species with similar structures and possible coexisting ones were tested along with nitrite. Among these, ferric ion is the only one that bring in some minor influence at even much higher concentration (1.0 μM), which was a reasonable due to its oxidative property. All other species show no obvious interference (Fig. 3). This kind of excellent selectivity might be attributed to the unique catalysis from nitrite during the process.

Analysis of water samples

To demonstrate the applicability of the developed method, water samples from different sources were analyzed. Tap water was provided by the water supply pipeline, lake water was collected from Dushuhu Lake (Suzhou, China), and rain water was from rainfall. All these samples were filtered using 0.22 μm filter, diluted with the double-distilled water. Then 200 μL of the processed practical samples were taken and analyzed according to the previous procedure. A recovery study was performed by adding a nitrite standard into the samples and measuring these with the same procedure. Satisfactory recoveries within the range from 96.5% to

Table 2 Results of the analyses of different water samples

Sample	NO_2^- detected/ μM	Standard added/ μM	Standard detected/ μM	Recovery/%	Spectrophotometry/ μM
Lake water	3.24 ± 0.29	1.00	1.04	104.0	3.47 ± 0.25
Rain water	0.514 ± 0.041	0.200	0.193	96.5	0.484 ± 0.037
Tap water	1.94 ± 0.17	0.600	0.587	97.8	2.10 ± 0.15

104.0% were obtained (Table 2). To further validate the reliability of the results, a reference spectrophotometric method was applied for the same samples [34] (detailed steps provided in the [Electronic Supporting Material](#)). The results obtained by the method are found in good accordance with those from the reference method (Table 2). Also an analysis on nitrite water for seasoning meat was also found satisfactory (Table S1). All these data indicate a high reliability and potential applicability of this method.

Conclusions

The catalytic property from nitrite was combined with the property of gold nanoclusters, and a sensitive means for nitrite detection was developed. Because of the catalysis from the analyte involved in the scheme, both high sensitivity and good selectivity were obtained. The practical applicability of this method was validated through successful detection of real samples. The studies have demonstrated that this method has a good potential for further practical applications.

Acknowledgements This work was supported by the National Natural Science Foundation of China (No. 21305100), the Project of Scientific and Technologic Infrastructure of Suzhou (SZS201708) and the Priority Academic Program Development of Jiangsu Higher Education Institutions (PAPD).

Compliance with ethical standards The authors declare that they have no competing interests.

References

- Lundberg JO, Gladwin MT, Ahluwalia A, Benjamin N, Bryan NS, Butler A, Cabrales P, Fago A, Feelisch M, Ford PC, Freeman BA, Frenneaux M, Friedman J, Kelm M, Kevil CG, Kim-Shapiro DB, Kozlov AV, Lancaster JR, Lefter DJ, McColl K, McCurry K, Patel RP, Petersson J, Rassaf T, Reutov VP, Richter-Addo GB, Schechter A, Shiva S, Tsuchiya K, van Faassen EE, Webb AJ, Zuckerbraun BS, Zweier JL, Weitzberg E (2009) Nitrate and nitrite in biology, nutrition and therapeutics. *Nat Chem Biol* 5:865–869. <https://doi.org/10.1038/nchembio.260>
- Cammack R, Joannou CL, Cui X, Martinez CT, Maraj SR, Hughes MN (1999) Nitrite and nitrosyl compounds in food preservation. *Biochim Biophys Acta* 1411:475–488. [https://doi.org/10.1016/S0005-2728\(99\)00033-X](https://doi.org/10.1016/S0005-2728(99)00033-X)
- Huang S, Li L, Mei L, Zhou J, Guo F, Wang A, Feng J (2016) Electrochemical sensor for nitrite using a glassy carbon electrode modified with gold-copper nanochain networks. *Microchim Acta* 183:791–797. <https://doi.org/10.1007/s00604-015-1717-z>
- Wang Q, Huang H, Ning B, Li M, He L (2015) A highly sensitive and selective spectrofluorimetric method for the determination of nitrite in food products. *Food Anal Methods* 9:1293–1300. <https://doi.org/10.1007/s12161-015-0306-4>
- Bharath G, Madhu R, Chen S, Veeramani V, Mangalaraja D, Ponpandian N (2015) Solvent-free mechanochemical synthesis of graphene oxide and Fe₃O₄-reduced grapheneoxide nanocomposites for sensitive detection of nitrite. *J Mater Chem A* 3:15529–15539. <https://doi.org/10.1039/c5ta03179f>
- Kumar A, Gonc JM, Sukeri A, Araki K, Bertotti M (2018) Correlating surface growth of nanoporous gold with electrodeposition parameters to optimize amperometric sensing of nitrite. *Sensors Actuators B Chem* 263:237–247. <https://doi.org/10.1016/j.snb.2018.02.125>
- Helaleh MI, Korenaga T (2000) Ion chromatographic method for simultaneous determination of nitrate and nitrite in human saliva. *J Chromatogr B* 744:433–437. [https://doi.org/10.1016/S0378-4347\(00\)00264-4](https://doi.org/10.1016/S0378-4347(00)00264-4)
- Shariati-Rad M, Irandoust M, Niazi F (2015) A sensitive spectrofluorimetric method for the determination of nitrite in agricultural samples. *Food Anal Methods* 8:1691–1698. <https://doi.org/10.1007/s12161-014-0045-y>
- Zhang H, Kang S, Wang G, Zhang Y, Zhao H (2016) Fluorescence determination of nitrite in water using prawn-shell derived nitrogen-doped carbon nanodots as fluorophores. *ACS Sens* 1: 875–881. <https://doi.org/10.1021/acssensors.6b00269>
- Manoj D, Saravanan R, Santhanalakshmi J, Agarwal S, Gupta VK, Boukherroub R (2018) Towards green synthesis of monodisperse Cu nanoparticles: an efficient and high sensitive electrochemical nitrite sensor. *Sensors Actuators B Chem* 266:873–882. <https://doi.org/10.1016/j.snb.2018.03.141>
- Chen L, Wang C, Yuan Z, Chang H (2015) Fluorescent gold nanoclusters: recent advances in sensing and imaging. *Anal Chem* 87:216–229. <https://doi.org/10.1021/ac503636j>
- Lan G, Huang C, Chang H (2010) Silver nanoclusters as fluorescent probes for selective and sensitive detection of copper ions. *Chem Commun* 46:1257–1259. <https://doi.org/10.1039/b920783j>
- Cao D, Fan J, Qiu J, Tu Y, Yan J (2013) Masking method for improving selectivity of gold nanoclusters in fluorescence determination of mercury and copper ions. *Biosens Bioelectron* 42:47–50. <https://doi.org/10.1016/j.bios.2012.10.084>
- Tao Y, Li M, Ren J, Qu X (2016) Metal nanoclusters: novel probes for diagnostic and therapeutic applications. *Chem Soc Rev* 47: 8636–8663. <https://doi.org/10.1039/c5cs00607d>
- Luo M, Di J, Li L, Tu Y, Yan J (2018) Copper ion detection with improved sensitivity through catalytic quenching of gold nanocluster fluorescence. *Talanta* 187:231–236. <https://doi.org/10.1016/j.talanta.2018.05.047>
- Li R, Xu P, Tu Y, Yan J (2018) Albumin-stabilized gold nanoclusters as viable fluorescent probes in non-titrimetric iodometry for the detection of oxidizing analytes. *Microchim Acta* 143:497–502. <https://doi.org/10.1007/s00604-015-1661-y>
- Yang Y, Han A, Li R, Fang G, Liu J, Wang S (2017) Synthesis of highly fluorescent gold nanoclusters and their use in sensitive analysis of metal ions. *Analyst* 142:4486–4493. <https://doi.org/10.1039/c7an01348e>
- Kermani HA, Hosseini M, Miti A, Dadmehr M, Zuccheri G, Hosseinkhani S, Ganjali MR (2018) A colorimetric assay of DNA methyltransferase activity based on peroxidase mimicking of DNA template Ag/Pt bimetallic nanoclusters. *Anal Bioanal Chem* 410:4943–4952. <https://doi.org/10.1007/s00216-018-1143-2>
- Xu H, Zhu H, Sun M, Yu H, Li H, Ma F, Wang S (2014) Graphene oxide supported gold nanoclusters for the sensitive and selective detection of nitrite ions. *Analyst* 140:1678–1685. <https://doi.org/10.1039/c4an02181a>
- Xiang G, Wang Y, Zhang H, Fan H, Fan L, He L (2018) Carbon dots based dual-emission silica nanoparticles as ratiometric fluorescent probe for nitrite determination in food samples. *Food Chem* 260:13–18. <https://doi.org/10.1016/j.foodchem.2018.03.150>
- Wang Y, Tan X, Xue J, Li G, Shi L, Yang H, Liu L, Zhou B, Xiao X (2011) Determination of trace formaldehyde in blood plasma by resonance fluorescence technology. *Anal Chim Acta* 690:234–239. <https://doi.org/10.1016/j.aca.2011.02.030>

22. Sheng L, Zhao Z, Su B, Tao C, Jing W (2017) Kinetic determination of lanthanum(III) by the catalytic effect on the oxidation of fluorescent safranin dyes with potassium bromate. *Anal Sci* 33: 1401–1405. <https://doi.org/10.2116/analsci.33.1401>
23. Bai LS, Chi ZH (2001) Kinetic spectrophotometric determination of nitrite by the catalytic oxidation of bromocresol purple with potassium bromate. *Chin. J Anal Chem* 29:926–929. <https://doi.org/10.3321/j.issn:0253-3820.2001.08.016>
24. Balasubramanian P, Settu R, Chen S, Chen T, Sharmila G (2018) A new electrochemical sensor for highly sensitive and selective detection of nitrite in food samples based on sonochemical synthesized calcium ferrite (CaFe_2O_4) clusters modified screen printed carbon electrode. *J Colloid Interface Sci* 524:417–426. <https://doi.org/10.1016/j.jcis.2018.04.036>
25. Wang X, Tan W, Ji H, Liu F, Wu D, Ma J (2018) Facile electrosynthesis of nickel hexacyanoferrate/poly(2,6-diaminopyridine) hybrids as highly sensitive nitrite sensor. *Sensors Actuators B Chem* 264:240–248. <https://doi.org/10.1016/j.snb.2018.02.171>
26. Huang S, Liu L, Mei L, Zhou J, Guo F, Wang A, Fen J (2016) Electrochemical sensor for nitrite using a glassy carbon electrode modified with gold-copper nanochain networks. *Microchim Acta* 183:791–797. <https://doi.org/10.1007/s00604-015-1717-z>
27. Lo HS, Lo KW, Yeung CF, Wong CY (2017) Rapid visual and spectrophotometric nitrite detection by cyclometalated ruthenium complex. *Anal Chim Acta* 990:135–140. <https://doi.org/10.1016/j.aca.2017.07.018>
28. Feng Z, Li Z, Zhang X, Shi Y, Zhou N (2017) Nitrogen-doped carbon quantum dots as fluorescent probes for sensitive and selective detection of nitrite. *Molecules* 22:2061–2071. <https://doi.org/10.3390/molecules22122061>
29. Zhang H, Kang S, Wang G, Zhang Y, Zhao H (2016) Fluorescence determination of nitrite in water using prawn-shell derived nitrogen-doped carbon nanodots as fluorophores. *ACS Sens* 1:875–881. <https://doi.org/10.1021/acssensors.6b00269>
30. Ren H, Fan WB, Yu L (2018) Polyethylenimine-capped CdS quantum dots for sensitive and selective detection of nitrite in vegetables and eater. *J Agric Food Chem* 66:8851–8858. <https://doi.org/10.1021/acs.jafc.8b01951>
31. Gu B, Huang L, Hu J, Liu J, Su W, Duan X (2016) Highly selective and sensitive fluorescent probe for the detection of nitrite. *Talanta* 152:155–161. <https://doi.org/10.1016/j.talanta.2016.01.059>
32. Liu Y, Xue H, Liu J, Wang Q, Wang L (2018) Carbon quantum dot-based fluorometric nitrite assay by exploiting the oxidation of iron(II) to iron(III). *Microchim Acta* 185:129. <https://doi.org/10.1007/s00604-018-2668-y>
33. Wang Q, Huang H, Ning B, Li M, He L (2016) A highly sensitive and selective spectrofluorimetric method for the determination of nitrite in food products. *Food Anal Methods* 9:1293–1300. <https://doi.org/10.1007/s12161-015-0306-4>
34. Wang L, Chen J, Chen H, Zhou C, Ling B, Fu J (2011) A sensitive fluorimetric method for determination of trace amounts of nitrite based on luminescence energy transfer. *J Lumin* 131:83–87. <https://doi.org/10.1016/j.jlumin.2010.09.003>

Publisher's note Springer Nature remains neutral with regard to jurisdictional claims in published maps and institutional affiliations.